Patterning of Polymeric/Inorganic Nanocomposite and Nanoparticle Layers

Mingtai Wang,* Hans-Georg Braun,* and Evelyn Meyer

Institute of Polymer Research Dresden, Hohe Strasse 6, D-01069 Dresden, Germany

Received June 18, 2002

Polymeric/inorganic nanocomposite dishes of hydrolyzed poly(styrene-*alt*-maleic anhydride) (HSMA) and TiO_2 were patterned on substrates by microcontact printing (μCP) of the dispersions of nanosized TiO_2 colloidal particles in HSMA solutions; the structure formation with respect to the μCP process was discussed. The orderly arranged HSMA/TiO_2 dishes are homogeneous in size. After removal of the polymer in the printed composite dishes by calcination, well-defined nanostructured TiO_2 layers are formed in the regions where the composite dishes appear. The printed composite dishes come from the dishlike composite aggregates transferred onto a substrate from a stamp surface. The drying of the dispersion droplets formed in a topographically controlled de-wetting of the dispersion on the stamp surface results in the dishlike aggregates, for which the pinning of the droplet contact line is of key importance. The diameter of the printed dishes is mainly determined by the stamp geometry, and not influenced remarkably by HSMA and/or TiO_2 concentrations. The component fractions mainly influence the heights of the dish rim and plate, the width of the dish rim, and the continuity of the plate within the rim.

1. Introduction

With miniaturization in materials science nanoparticles are regarded as promising for the design of highly efficient optical and electronic devices because of their unique optical[1] and electronic[2] properties. For a number of future or existing applications, as light-emitting (LE) diode arrays on flat panels, for example, nanoparticle aggregates need to be ordered on a micrometer scale. Many methods, therefore, have been developed for patterning of nanoparticles, including template patterns created with photolithography,[3] microcontact printing (μCP)[4] or a conductive atomic force microscopy (AFM) tip[5] for the precipitation of nanoparticles from solutions, and micromolding[6] of nanosized colloid dispersions. As a soft lithography, μCP has substantially extended micro- and nanostructuring technology for the prepara-

tion of patterned surfaces.[7] However, in patterning nanoparticle aggregates μCP has been mainly applied to create pattern templates for the growth of nanoparticle layers,[4] where functionalized self-assembled monolayers that can initiate the nanostructure formation on interfaces are transferred onto substrates to form template areas. To our knowledge, only one study[8] related to the use of μCP to directly print nanoparticles has been done, which may be due to the difficulty in forming homogeneous nanoparticle layers on the tops of the extruding parts (i.e., protrusions) of the stamp that is generally prepared from poly(dimethylsiloxane) (PDMS).

In previous work[9] we demonstrated a new variant of μCP, which is termed micro-fluid-contact printing (μFCP), for the transfer of polymer dots of a spherical shape to a variety of surfaces. In the μFCP of a polymer, a PDMS stamp impregnated with the polymer solution is exposed to a gas stream to remove the excess polymer solution

* To whom correspondence should be addressed.Tel.: 0049-351-4658547. Fax: 0049-351-4658284. E-mails: mingtaiwang@hotmail.com (Wang); braun@ipfdd.de (Braun).

(1) (a) Mulvaney, P. *Langmuir* **1996**, *12*, 788. (b) Schaaff, T. G.; Shafigullin, M. N.; Khoury, J. T.; Vezmar, I.; Whetten, R. L.; Cullen, W. G.; First, P. N.; Gutiérrez-Wing, C.; Ascensio, J.; Jose-Yacamán, M. J. *J. Phys. Chem. B* **1997**, *101*, 7885. (c) Alivisatos, A. P. *J. Phys. Chem.* **1996**, *100*, 13226.

(2) (a) Khairutdinov, R. F. *Colloid J.* **1997**, *59*, 535. (b) Lee, T.; Liu, J.; Chen, N.-P.; Andres, R. P.; Janes, D. B.; Reifenberger, R. *J. Nanopart. Res.* **2000**, *2*, 345.

(3) (a) Ha, K.; Lee, Y.-J.; Chun, Y. S.; Park, Y. S.; Lee, G. S.; Yoon, K. B. *Adv. Mater.* **2001**, *13*, 594. (b) Liu, J.-F.; Zhang, L.-G.; Gu, N.; Ren, J.-Y.; Wu, Y.-P.; Lu, Z.-H.; Mao, P.-S.; Chen, D.-Y. *Thin Solid Films* **1998**, *327−329*, 176. (c) Vossmeyer, T.; Delonno, E.; Heath, J. R. *Angew. Chem., Int. Ed. Engl.* **1997**, *36*, 1080. (d) Dressick, W. J.; Dulcey, C. S.; Brandow, S. L.; Witschi, H.; Neeley, P. F. *J. Vac. Sci. Technol. A* **1999**, *17*, 1432. (e) Brandow, S. L.; Chen, M.-S.; Aggarwal, R.; Dulcey, C. S.; Calvert, J. M.; Dressick, W. J. *Langmuir* **1999**, *15*, 5429. (f) Collins, R. J.; Shin, H.; DeGuire, M. R.; Heuer, A. H.; Sukenik, C. N. *Appl. Phys. Lett.* **1996**, *69*, 860. (g) Sugimura, H.; Hozumi, A.; Kameyama, T.; Takai, O. *Adv. Mater.* **2001**, *13*, 667.

(4) (a) Palacin, S.; Hildber, P. C.; Bourgoin, J.-P.; Miramond, C.; Fermon, C.; Whitesides, G. M. *Chem. Mater.* **1996**, *8*, 1316. (b) Clem, P. G.; Jeon, N. -L.; Nuzzo, R. G.; Payne, D. A. *J. Am. Ceram. Soc.* **1997**, *80*, 2821. (c) Qin, D.; Xia, Y.; Xu, B.; Yang, H.; Zhu, C.; Whitesides, G. M. *Adv. Mater.* **1999**, *11*, 1433. (d) Bechinger, C.; Muffler, H.; Schäfle, C.; Sundberg, O.; Leiderer, P. *Thin Solid Films* **2000**, *366*, 135. (e) Chen, C.-C.; Lin, J.-J. *Adv. Mater.* **2001**, *13*, 136. (f) Ji, J.; Li, X.; Canham, L. T.; Coffer, J. L. *Adv. Mater.* **2002**, *14*, 41.

(5) Mesquida, P.; Stemmer, A. *Adv. Mater.* **2001**, *13*, 1395.

(6) (a) Seraji, S.; Wu, Y.; Jewell-Larson, N. E.; Forbess, M. J.; Limmer, S. J.; Chou, T. P.; Cao, G. *Adv. Mater.* **2000**, *12*, 1421. (b) Huang, L.; Wang, Z.; Sun, J.; Miao, L.; Li, Q.; Yan, Y.; Zhao, D. *J. Am. Chem. Soc.* **2000**, *122*, 3530.

(7) Xia, Y.; Rogers, J. A.; Paul, K. E.; Whitesides, G. M. *Chem. Rev.* **1999**, *99*, 1823.

(8) Hidber, P. C.; Helbig, W.; Kim, E.; Whitesides, G. M. *Langmuir* **1996**, *12*, 1375.

(9) Wang, M.; Braun, H.-G.; Kratzmüller, T.; Meyer, E. *Adv. Mater.* **2001**, *13*, 1312.

on the stamp surface, and dotlike polymer aggregates rapidly form on the stamp protrusion tops; the dotlike polymer aggregates are transferred onto a substrate by contacting. The μFCP differs from the conventional μCP in that the transferred aggregates are not solvent-free but still contain some solvent during the transfer process and that the size of transferred objects is much smaller than the scale of the stamp protrusion surfaces. As a polymer solution of hydrolyzed poly(styrene-*alt*-maleic anhydride) (HSMA) in THF was dispersed with nanosized TiO_2 colloidal particles and used as the ink for the μFCP process, HSMA/TiO_2 layers with a dish shape were printed on substrates, resulting in patterning of nanocomposite layers. After removal of the polymer in the printed composite dishes, the patterns of nanostructured TiO_2 layers were left behind on the substrates. Our findings are expected to find applications in materials science. In the present paper, we demonstrate the application of μFCP for patterning nanostructured materials and describe the principle characteristics with respect to the structure formation in μFCP of polymer/nanoparticle dispersions.

2. Experimental Section

Preparation of Composite Ink Dispersion. Poly(styrene-*alt*-maleic anhydride) copolymer (SMA) ($M_n = 2560$, $M_w/M_n = 1.04$) was used as the precursor of hydrolyzed SMA (i.e., HSMA), and HSMA solution was made from the SMA solution (3 mg/mL) in THF by the procedure described previously.[9]

Nanosized TiO_2 colloidal dispersion was prepared by the hydrolysis of $TiCl_4$ in 6 M HCl as described in the literature,[10] where the particle sizes were reported in the range from 2 to 4 nm. $TiCl_4$ (99%, Fluka) was slowly added dropwise to 6 M HCl under vigorous stirring at ambient temperature to make the solution of 0.5 M $TiCl_4$. Heating the $TiCl_4$ solution, which had been filtered to eliminate the possible impurities, at 80 °C for 4 h gave a transparent TiO_2 colloidal dispersion that was observed to be stable at least for 4 months. The TiO_2 amount in the colloidal dispersion was calculated based on the assumption that all the $TiCl_4$ molecules hydrolyzed into TiO_2 according to eq 1.

$$TiCl_4 + 2H_2O = TiO_2 + 4HCl \qquad (1)$$
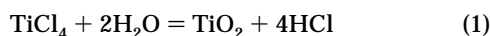
The TiO_2 colloidal dispersion was added into the HSMA solution with a certain weight ratio of SMA/TiO_2; the mixture dispersion was adjusted with THF to a defined concentration and stirred at room temperature for 2 h. Since HSMA has a high content of carboxylic acid groups, the interaction between the organic chains and the inorganic particle surface is strong,[11] so HSMA is easily adsorbed onto the particle surfaces and stabilizes the particles in the mixture dispersion. The as-obtained composite dispersions, which were transparent and observed to be stable for at least 2 months without precipitation at ambient temperature, were used as inks for μFCP processes. The total concentration of an ink dispersion (C_{total}) was expressed by the weight of SMA and TiO_2 per milliliter of the dispersion.

μFCP Process and Sample Characterization. In the present study the Si wafer was used as the substrate for μFCP. Besides the Si wafer the composite dishes can be reproducibly printed on other substrates such as a glass slide, polymer film, and gold surface. Si wafers were first ultrasonically treated for 20 min in aqueous detergent solution, acetone, alcohol, and deionized water, respectively; then after being washed extensively with deionized water, the cleaned substrates were kept
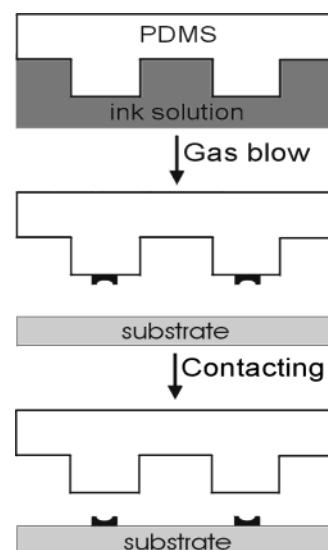
(10) Liu, Y.; Wang, A.; Claus, R. *J. Phys. Chem. B* **1997**, *101*, 1385.
(11) Kotov, N.; Dékány, I.; Fendler, J. H. *J. Phys. Chem.* **1995**, *99*, 13065.


Figure 1. Schematic illustration of our approach.

in absolute alcohol for use. The hexagonally structured PDMS stamps (stamp 1 and 2) used in this study had the same geometrical features as those we described previously.[9] Briefly, the radii, R, for the internal tangent circles of every hexagonal protrusion surface are $5\sqrt{3}$ μm (stamp 1) and $\sqrt{3}$ μm (stamp 2); and four adjacent protrusions on the stamp 1 and stamp 2 surfaces form a repeat rectangle unit of 25×29 and 5×5.8 μm^2, respectively.

The substrate and stamp surfaces were rinsed with absolute ethanol and dried in a nitrogen stream before use. The stamp (about 4.5×4.5 mm) that was stuck to a small metal holder (for example, a SEM sample holder) for convenient use was impregnated with an ink dispersion for 15−20 s, and then it was briefly held in a stream of nitrogen to remove the excess dispersion on the stamp surface and further dried freely in the air for about 1 min. The as-inked stamp was brought into contact with a substrate for about 60 s under 100−150 g of external force over the stamp surface, and the composite dishes were transferred onto the substrate when the stamp was carefully peeled off. The contacting process was carried out on an electronic balance with an accuracy of 0.01 g, and the hand-added external force was monitored by the balance. The external pressure was imposed upon the stamp surface to obtain close contact between the stamp and substrate.

Video recording under a light microscope, scanning electron microscopy (SEM), and AFM measurements were carried out as described previously.[9] The energy dispersion X-ray (EDX) analysis was conducted with a Tracor Voyager system on the same scanning electron microscope (LEO Gemini DSM 982 SEM) as in the SEM measurements, but the sample was coated with a 5−6-nm carbon layer to enhance the conductivity.

3. Results and Discussion

3.1. Patterning of Nanocomposite and Nanoparticle Layers by μFCP. As a variant of microcontact printing (μCP) to transfer microstructured objects, μFCP has allowed HSMA dots to be transferred onto a variety of substrates.[9] As the HSMA solution was dispersed with nanosized TiO_2 colloidal particles and used as the ink for the μFCP process, HSMA/TiO_2 nanocomposite layers were printed on substrates. However, the composite layers are of a dish shape instead of a spherical cap shape. In our approach (Figure 1), dishlike composite aggregates first form on a stamp surface (refer to the later text), then they are transferred onto a substrate by contacting, and finally the composite dishes
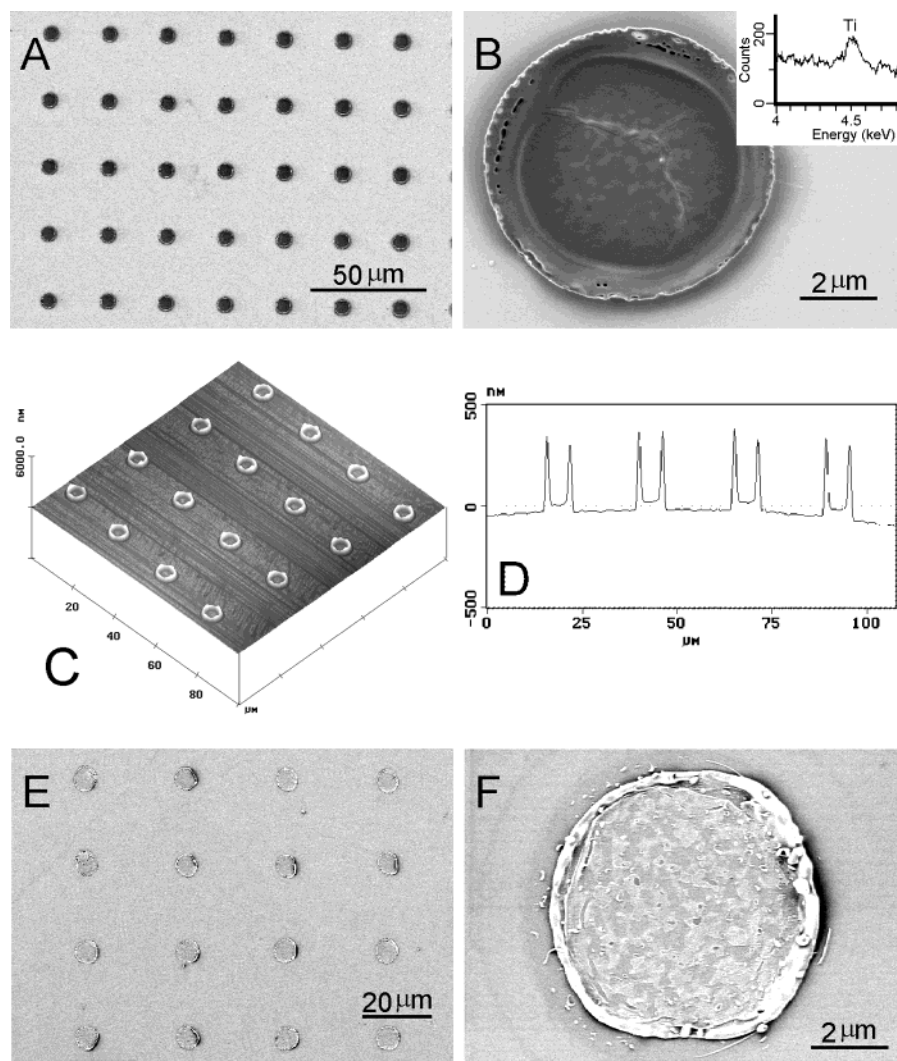
Figure 2. SEM (A, B) and contact-mode AFM (C) images for the HSMA/TiO$_2$ nanocomposite dishes printed on a Si wafer, (D) the AFM sectional view along a dish alignment in image (C), and (E, F) SEM images of the derived nanostructured TiO$_2$ layers after removal of polymer in the composite dishes (A or C) by calcination. The inset to (B) is the EDX spectrum for one of the printed dishes. The diameter and the rim width of the TiO$_2$ layers were about 6.8 and 0.4 μm, respectively; AFM shows that the peripheral rims and the plates within the rims of the TiO$_2$ layers were about 80−130 and 10 nm in height, respectively. In the experiments, stamp 1 and a composite dispersion of 4 mg/mL with a weight ratio of SMA/TiO$_2$ of 3/1 were used. To remove the polymer, the printed dishes were calcinated in air at 500 °C for 4 h (heating rate, 6 °C/min).

result from the transferred dishlike aggregates on the substrate after solvent evaporation.

The HSMA/TiO$_2$ composite dishes printed by μFCP were characterized with SEM and AFM. In Figure 2, one can see the well-defined order of the printed dishes, and four adjacent dishes form a rectangle of 25 × 29 μm^2, corresponding to the periodicity of the protrusions of the used stamp (Figure 2A,C). The magnified SEM image (Figure 2B) clearly shows the profile of the printed dishes. Both SEM and AFM data show that the diameters of the dishes are very homogeneous, and AFM sectional views (Figure 2D) show that both the rims and the plates within the rims of the dishes are also quite homogeneous in height. The dimensional parameters of the printed dishes are listed in Table 1. EDX analysis of the printed dishes verifies that they contain TiO$_2$ component, as shown by the Ti signal at 4.5 keV in the EDX spectrum (inset to Figure 2B). After removal of the polymer in the printed dishes by calcination, well-defined nanostructured TiO$_2$ layers were obtained on the substrate (Figure 2E), where more TiO$_2$ particles

accumulated in the peripheral locations of the dishes as revealed by the magnified SEM images of TiO$_2$ layers (Figure 2F) and AFM data. The periodicity of the derived TiO$_2$ layers is identical to that of the printed dishes. Known from SEM and AFM results, the composite and TiO$_2$ layers do look not very even, especially in the rim regions, which indicates that the nanoparticle agglomeration still existed to some extent in the dispersion.

As is well-known, polymer matrixes have received great attention in preparation of nanostructured materials, for they can prevent the serious agglomeration of nanoparticles that results from their high specific surface area and provide a polymeric/inorganic nanocomposite system with both useful functionality and mechanical integrity.[12] These polymeric/inorganic nanocomposites are generally prepared by coprecipitation from the dispersion of nanoparticles in polymer solu-

(12) (a) Zhang, J.; Wang, B.; Ju, X.; Liu, T.; Hu, T. *Polymer* **2001**, *42*, 3697. (b) Gao, M.; Richter, B.; Kirstein, S. *Adv. Mater.* **1997**, 9, 802.

Table 1. Dimensional Parameters of the Dishes Obtained from Different Ink Dispersions[a]

C_{total}[b] (mg/mL)	weight ratio[c] (SMA/TiO$_2$)	TiO$_2$ fraction[c] (mg/mL)	HSMA fraction[c] (mg/mL)	average dish dimensional parameters		
				diameter (μm)	rim width/ height (μm)	plate height (nm)
4.0	3/1	1.0	3.0	7.0[d]	1.1/0.45	40
2.0	4/1	0.4	1.6	7.0[d]	1.0/0.40	35
0.5	4/1	0.1	0.4	7.1[d]	0.5/0.15	often broken[g]
0.9	0.8/1	0.5	0.4	6.8[d]	0.3/0.16	20
1.0	4/1	0.2	0.8	1.1[e]	0.15/0.12	15
1.15	1.8/1	0.4	0.75	6.8[f]	1.0/no data	no data

[a] The average parameters were obtained from the images in Figures 2−4. [b] Total concentration of ink dispersion. [c] In ink dispersion. [d] Printed with stamp 1. [e] Printed with stamp 2. [f] On the surface of stamp 1. [g] A broken plate was not homogeneous in height; its thickness was about 5−26 nm.

tions or by colloid synthesis of nanoparticles with polymers in situ or added afterward.[13] This synthetic scenario offers the possibility to use μFCP to pattern many of these nanocomposites. On the other hand, as colloid chemistry is particularly a very suitable approach to nanostructured materials, where colloidal aggregates can serve as containers or templates for the in situ generation and subsequent stabilization of nanoparticles,[14] it is expected that many nanoparticle layers (in particular, oxides) may be patterned by the μFCP process using a suitable polymer carrier, for which the patterning of nanostructured TiO$_2$ layers is a good example (Figure 2E,F).

3.2. μFCP of Nanodispersions in Polymer Solutions. 3.2.1. Structure Formation on Stamp Surface. As shown by Figure 1, the formation of dishlike composite aggregates on stamp protrusion surfaces is the key step for the structure formation in our approach. To reveal the formation of the dishlike composite aggregates, the drying process of the composite dispersion on a stamp surface was recorded under a light microscope by a video system. Analysis of the video sequences gave the details of a topographically controlled de-wetting of the composite dispersion on the stamp surface: after removal of the excess dispersion by a nitrogen stream, the dispersion layer on the stamp surface breaks up due to the topography of the stamp surface; one part of the ruptured liquid layer appears on the protrusion tops, while the rest gathers within the capillary spacings between the protrusions. These processes are the same as those in the cases of pure polymer solutions; one can refer to our previous report[9] for the documentation. We focus here on the behaviors of the ruptured liquid layers on protrusion surfaces.

The drying of the dispersion layers on every protrusion surface is obviously the origin of forming dishlike aggregates, and it was revealed to proceed mainly by stages I and II, as shown by the plot in Figure 3. In drying stage I, the dispersion layer on each protrusion surface de-wetted to its center within a few seconds with the size of its wetting area reduced rapidly and formed a droplet at the central point of the surface (Figure 3A). The centralization of the dispersion droplets on every protrusion surface is due to the deformation of the protrusion surfaces as a result of the inhomogeneous
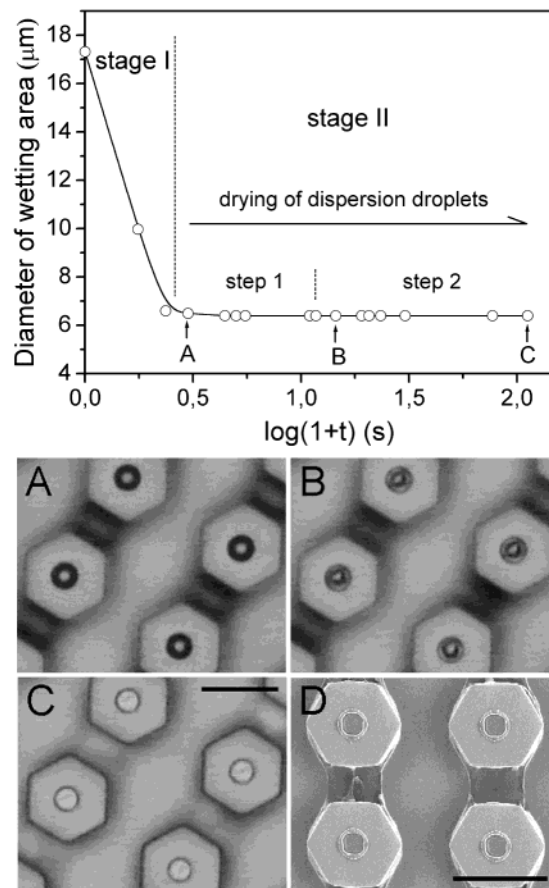
(13) (a) Spatz, J. P.; Herzog, T.; Mössmer, S.; Ziemann, P.; Möller, M. *Adv. Mater.* **1999**, *11*, 149. (b) Caseri, W. *Macromol. Rapid Commun.* **2000**, *21*, 705. (c) Mayer, A. B. R. *Polym. Adv. Technol.* **2001**, *12*, 96.

(14) (a) Fendler, J. H.; Meldrum, F. C. *Adv. Mater.* **1995**, *7*, 607. (b) Lin, J.; Siddiqui, J. A.; Ottenbrite, R. M. *Polym. Adv. Technol.* **2001**, *12*, 285.

Figure 3. Plot for the wetting area of the composite dispersion on stamp protrusion tops vs time (t) during drying. The optical microscopic images (A−C) correspond to the drying time, points A, B, and C in the plot, and SEM image (D) was taken after the sample with ringlike morphology (C) had been dried additionally for 30 min in air under a light microscope. An experiment was done on the surface of stamp 1, and 1.15 mg/mL composite dispersion with a weight ratio of SMA/TiO$_2$ of 1.8/1 was applied. The scale bar for all the optical microscopic images is 17 μm (C), but that for the SEM image is 20 μm (D). **Note**: the time when the dispersion layer on the stamp surface broke up is taken as 0.0 s; the wetting area on each protrusion surface is expressed by the diameter of the droplet on it, and the initial size of the wetting area at $t = 0.0$ s is expressed by the $2R$ value of the stamp ($R = 5\sqrt{3}$ μm).

swelling in the short contact time between the protrusions and solvent, which creates concave protrusion surfaces and causes the dispersion on them to de-wet to their central points, as has been demonstrated privously.[9] In drying stage II, about 10 s later since formation the profile of the droplets under the light microscope changed with their peripheral edges fixed

and the dispersions within the peripheral edges shrinking (Figure 3B), and finally a ringlike morphology was given (Figure 3C). No noticeable changes were observed when the ringlike morphology in Figure 3C was kept additionally for 30 min under the light microscope. SEM at low voltage revealed that the ringlike composite aggregates on the stamp surface under the light microscope (Figure 3C) were virtually in a dish shape, as shown by Figure 3D. Note that the dishes on the stamp surface (Figure 3D) did not contain solvent when imaged with SEM, but they undoubtedly did result from the dishlike aggregates that formed during the drying process of the composite dispersion on the stamp surface. It can be seen that the dishlike composite aggregates (Figure 3C) or the composite dishes (Figure 3D) are much smaller in diameter than the protrusions themselves and locate at the centers of every protrusion surface. Obviously, the centralization of dishlike aggregates on every protrusion surface ensures the spaces between the printed dishes on the substrate to be strictly defined by the stamp geometry.

The formation of the droplets on a stamp surface, that is, drying stage I, happens very fast, but the profile changes of them (stage II) proceed relatively slowly. Because the ink on the stamp surface contained nanoparticles, the common principles governing the drying of particle-containing droplets are inevitably involved in our cases. In the drying of a droplet containing dispersed solid particles, a ringlike deposition of the solids along the perimeter is always the case, which is shown by the brown ring left when a drop of coffee dries on a solid surface.[15,16] It is concluded from the previous studies[15,16] that a capillary flow inside the drying droplet ensures that liquid evaporating from the three-phase contact line is replenished by liquid from the interior and keeps the contact line of the droplet fixed to its initial position in which the outward flow inside the droplet carries the dispersed solids to its contact line where the accumulated solids perpetuate the pinning of the contact line and form a ringlike deposit that remains after all the liquid evaporates. The ringlike deposition has been applied to the generation of nanoparticle rings on substrates.[17] We believe that the formation of the droplets on protrusion surfaces (stage I) is due to the surface energy of the isolated liquid layers, but the change of the dispersion droplets into dishlike aggregates during drying (stage II) is related to the pinning of the contact line.[15-17]

After the dispersion layer on a stamp surface broke up, the isolated thin dispersion layer on a protrusion surface was energetically unstable; it changed rapidly into a height profile that had a spherical cap shape dictated by surface tension, resulting in the fast formation of an equilibrium droplet of minimum energy. In drying stage I, the effect of the surface tension of the thin liquid layer on a protrusion surface suppressed the contributions to the pinning of its contact line from both the friction on the surface close to the contact line of

the liquid layer and the outward flow inside the liquid,[18] leading to the shrinking of the contact line to the position of an equilibrium dispersion droplet (Figure 3A). Since the formation of the equilibrium droplets on the protrusion surfaces, the drying of them in stage II proceeded as common droplets containing dispersed solids, where the contact line of such a droplet was pinned at its initial position, and many dispersed nanoparticles, with adsorbed polymer chains on their surfaces, were carried by the outward flow inside the droplet to the droplet contact line, leading to the formation of a high peripheral rim (Figure 3C,D).

The drying process of the dispersion droplets (stage II) can be further divided into two steps, step 1 and step 2, as depicted by the plot in Figure 3. Step 1 lasted for ≈10 s in the tested samples, but step 2 lasted for a longer time. According to the description from ref 17, step 1 corresponds to the growth of the dish rim, where the rim height and width are increasing while the droplet profile is flattening, and the covering layer on the composite droplet surface formed by the polymer precipitated during solvent evaporation can prevent the fast evaporation of solvent from inside the droplet and facilitate the growth of the dish rim; step 2 corresponds to the shrinkage of dispersion after detachment of the contact line from the dish rim when the dispersion inside the droplets is not sufficient to maintain the old cap shape. After the detachment of the contact line, the growth of the dish rim is practically stopped;[17] the solutes in the shrinking dispersion precipitate and form the dish plate within the peripheral rim (refer to later discussions). The rim growth time, that is, the time for the drying step 1 of dispersion droplets, is affected by the droplet volume. Previous data[17] show the time for the growth of a ring of 0.1-cm radius in drying a 0.3-μL suspension droplet is about 100 s, and the growth time of about 1300 s indicates a much larger droplet and ring.[15] The dish/rim formed on each protrusion surface of stamp 1 (Figure 3D) has a diameter of around 7 μm; the time for it to grow was observed to be about 10 s. Given the dispersion droplet on a protrusion surface of stamp 1 is a half-sphere of 7-μm diameter, the volume of the assumed droplet is about 9×10^{-8} μL, which is much smaller than those compared here.[15,17] Of course, the rim growth time is also influenced by the viscosity and solvent evaporation rate in the droplet.

3.2.2. Dimensions of the Printed Dishes. After a short time since formation (≈1-2 min, refer to the Experimental Section), the dishlike aggregates on a stamp surface were transferred onto a substrate by contacting the stamp surface with the substrate, and the transferred composite aggregates became rigid composite dishes on the substrate after the complete evaporation of the solvent inside them. During the transfer process the dishlike aggregates still contained some solvent and were not rigid; otherwise, the printed dishes on the substrate should be reverse in shape to the dishes on the stamp surface. The fact that the difference between the diameters of the dishes on the stamp 1 surface (Figure 3 D) and on the substrate (Figure 2) is very small indicates that the dimensions of the dishlike aggregates almost remain unchanged

(15) Deegan, R. D.; Bakajin, O.; Dupont, T. F.; Huber, G.; Nagel, S. R.; Witten, T. A. *Nature* **1997**, *389*, 827.
(16) Deegan, R. D. *Phys. Rev. E* **2000**, *61*, 475.
(17) Maenosono, S.; Dushkin, C. D.; Saita, S.; Yamaguchi, Y. *Langmuir* **1999**, *15*, 957.

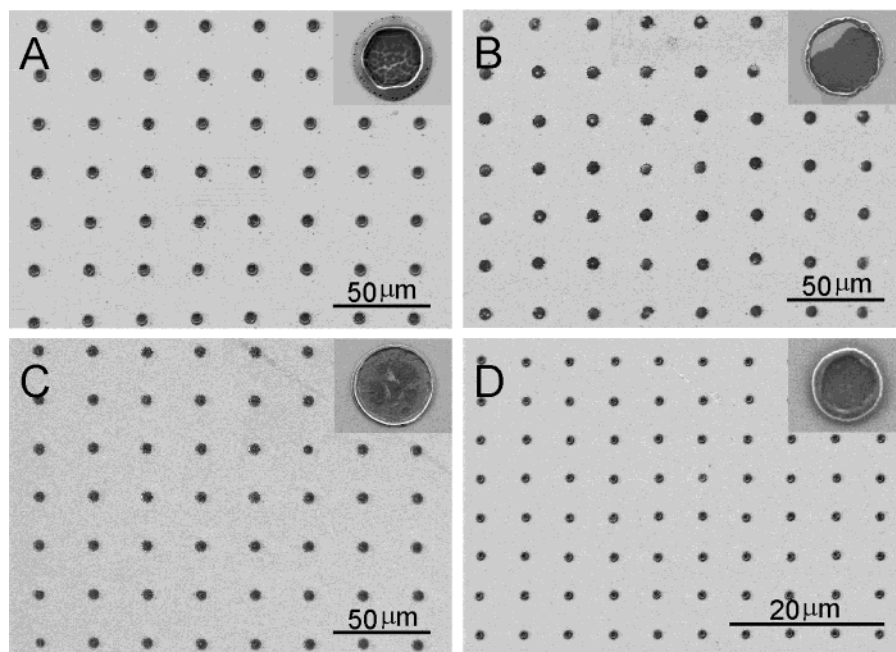(18) Adachi, E.; Dimitrov, A. S.; Nagayama, K. *Langmuir* **1995**, *11*, 1057.

Figure 4. SEM images for HSMA/TiO$_2$ nanocomposite dishes printed on Si wafers with different dispersions and stamps. The dishes were printed with stamp 1 (A−C) and stamp 2 (D). The ink dispersions had concentrations of 2.0 mg/mL (A), 0.5 mg/mL (B), and 1.0 mg/mL (D) and a weight ratio of SMA/TiO$_2$ of 4/1 (A, B, D), but a composite dispersion of 0.9 mg/mL with a weight ratio of SMA/TiO$_2$ of 0.8/1 was used to print dishes in image (C). The dishes in every image were typically shown by the corresponding SEM images inset.

during the transfer process. Hence, the formation process of the dishlike aggregates on a stamp surface can be reasonably evaluated with the data obtained from the printed dishes.

Table 1 summarizes the average dimensional parameters of the printed dishes from different dispersions. The diameter of a printed dish virtually comes from the initial volume of the dispersion droplet on each stamp protrusion surface. Even though the precise volume of the initial isolated dispersion layer on a stamp protrusion surface cannot be measured experimentally, it must depend on the scale of the protrusion surface. Under the same experimental conditions (e.g., ambient temperature and moisture, nitrogen gas pressure, and blowing time when removing the excess dispersion on the stamp surface), the height of the initial layers of the different dispersions left on the same-sized stamp protrusions after exposure to a nitrogen stream can be estimated to be equal. Therefore, the initial isolated layers of the different ink dispersions on the same protrusion surfaces will be of an equal volume, leading to the same-sized initial droplets. As a result of the pinning of the contact line in drying the initial droplets, the dishlike composite aggregates on the same stamp surface resulted from the different ink dispersions should be of almost a similar diameter, which further ensures the dishes printed from them will have a similar diameter as well. This expectation was confirmed by our experimental results, as shown by Figure 4 and the data in Table 1. The dishes printed with stamp 1 and ink dispersions of different component concentrations always had a diameter of about 7 μm in the tested range. However, a smaller stamp (i.e., stamp 2) may cause a pronounced reduction in dish diameter. So the diameter of the printed dishes on a substrate is mainly predetermined by the stamp geometry, but not influenced remarkably by HSMA and/or TiO$_2$ concentrations. Obvi-

ously, the diameter of the further derived TiO$_2$ layers also depends mainly on the stamp geometry.

Except for the diameter, the rim width and height and the plate height are also important parameters. As the rims form ahead of the plates in the formation of dishes, the rim growth will significantly influence the plate and whole dish dimension; hence, the rim size is a much more efficient parameter than others in evaluating the formation of the dishlike aggregates on stamp surfaces. Generally known from Table 1, a higher particle concentration leads to a higher and thicker dish rim, which agrees well with the results of others.[15,16] However, the influence of particle fractions on rim growth is often affected by the polymer in dispersion. During drying of the dispersion droplets, the polymer can affect the particle motion during the rim growth, by changing the viscosity of the dispersion and by changing the evaporation rate of the solvent in the droplets when the precipitated polymer forms covering layers on the droplet surfaces. These two effects will be competitive factors in affecting the rim growth, as is shown by our results.

Even though TiO$_2$ particle concentrations are quite different, the width and height of the rims in Figure 2A (C_{total} = 4.0 mg/mL, SMA/TiO$_2$ = 3/1) do not differ greatly from those in Figure 4A (C_{total} = 2.0 mg/mL, SMA/TiO$_2$ = 4/1). We think that in these two cases the viscosity is the dominant factor in affecting the rim growth. The dispersion for Figure 2A had a higher viscosity due to the higher polymer fraction (Table 1) than that for Figure 4A; the ability for the particles to move around during rim growth in the former case was consequently reduced, resulting finally in a rim size similar to that in Figure 4A. On the other hand, the TiO$_2$ fraction for Figure 4C (C_{total} = 0.9 mg/mL, SMA/TiO$_2$ = 0.8/1) is comparable to that for Figure 4A, but the rim size in Figure 4C is much smaller than that in

Figure 4A. This result indicates the effect of the solvent evaporation rate on the rim growth. As an ink dispersion contains a high polymer fraction, an efficient polymer covering layer can be easily formed on the droplet surface to prevent fast solvent evaporation. However, as the dispersion contains a much lower polymer fraction, it will take a longer time to form an efficient polymer covering layer on the dispersion droplet surface, and the solvent inside the droplet evaporates more easily. Due to the faster evaporation rate of solvent inside the dispersion droplets for Figure 4C, the growth of the rim was limited to a smaller scale.

As illustrated (Figure 3) and described in the text, the dish plate within the rim forms in drying step 2 of a dispersion droplet after the detachment of the contact line. Generally, the higher the ink concentration, the higher the plate thickness in the printed dishes (Table 1). But a very low TiO_2 concentration can lead to broken plates on a substrate, and the breaking often starts from the rim, as shown by Figure 4B ($C_{total} = 0.5$ mg/mL, $SMA/TiO_2 = 4/1$). Two processes are possible to produce the broken plates on a substrate. One is that the broken plates on a substrate come directly from the dishlike aggregates with broken plates on a stamp surface; the other is that they are produced in the transfer process, where some plate parts in the dishlike aggregates are too thin to be strong enough and are broken or detached from the rim during the transfer process. Considering the polymer fraction and the rim size in Figure 4B are comparable with Figure 4C where no broken plates are found, we tend to take the first possibility as the origin for our results in Figure 4B because if the second possibility were the main reason, the broken plates would also be found in Figure 4C. In the shrinking of the dispersion after the detachment of the contact line from the dish rim (step 2), a plate will form within the peripheral rim, depending on the competition between further pinning of the contact line and the de-wetting of the remaining dispersion on the protrusion surface due to surface tension. This competition phenomenon has been manifested in the drying of particle-containing droplets[16] by the formation of a cellular pattern within the solid ring, for example. The TiO_2 particle fraction for Figure 4B was very low; some segments of the contact line of the remaining dispersion switched to a de-pinning state after detachment of the contact line from the dish rim, and the dispersion de-wetted to the position where the contact line was pinned again. De-wetting in step 2 creates the broken plates in Figure 4B, which can be restricted by increasing the particle fraction in ink (Figure 4C).

4. Conclusion

μCP is a possible method for patterning the polymeric/inorganic nanocomposite and, further, the pure inorganic layers on a substrate. But the printed composite layers are of a dish shape, and more nanoparticles accumulate in the peripheral locations of the dishes. In the μCP process, dishlike $HSMA/TiO_2$ aggregates first form on a stamp surface and are then transferred to a substrate by contacting the stamp with the substrate when they still contain some solvent; finally, rigid $HSMA/TiO_2$ dishes result from the transferred dishlike aggregates after complete solvent evaporation. The dishlike aggregates originate from the drying of dispersion droplets that are formed on the stamp surface by a topographically controlled de-wetting of the dispersion there. The diameter of the printed $HSMA/TiO_2$ dishes, and the derived TiO_2 layers after calcination, is mainly determined by the stamp geometry and not influenced remarkably by HSMA and/or TiO_2 concentrations. The growth of dish rims depends on the component fractions in ink dispersions; a higher TiO_2 particle concentration generally leads to a larger rim, but the polymer imposes influences on the rim growth by changing the viscosity and the solvent evaporation rate in the dispersion droplets. The thickness of printed dish plates mainly increases with the total concentration of ink, but a very low particle fraction in ink often leads to broken plates within the dish rims.

CM021237S